JOURNAL OF CULTURAL ANALYSIS AND SOCIAL CHANGE

Journal of Cultural Analysis and Social Change,
2025, 10(4), 1766-1780
ISSN: 2589-1316

Modeling to COVID-19 Mortality Data: Using the Neutrosophic Gompertz Inverse Rayleigh Model with Estimation

Alaa A. ELnazer[1*], Raghad W. Faris[2], Nooruldeen Ayad Noori [3], Ehab M. Almetwally[4], Mohammed Elgarhy[5]

[1] *Department of Marketing, College of Business, Imam Mohammad Ibn Saud Islamic University (IMSIU), Riyadh 11432, Saudi Arabia; aaelnazer@imamu.edu.sa*
[2] *Mathematics department, College of Education for Women, Tikrit University, Iraq; rwamedh@tu.edu.iq*
[3] *Anbar Education Directorate, Anbar, Iraq; Nooruldeen.a.noori35508@st.tu.edu.iq*
[4] *Department of Mathematics and Statistics, College of Science, Imam Mohammad Ibn Saud Islamic University (IMSIU), Riyadh, Saudi Arabia; emalmetwally@imamu.edu.sa*
[5] *Department of Basic Sciences, Higher Institute of Administrative Sciences, Belbeis, AlSharkia, Egypt; dr.moelgarhy@gmail.com*
[5] *Department of Computer Engineering, Biruni University, 34010, Istanbul, Turkey; dr.moelgarhy@biruni.edu.tr*

***Corresponding Author:** aaelnazer@imamu.edu.sa

Citation: ELnazer, A. A., Faris, R. W., Noori, N. A., Almetwally, E. M. & Elgarhy, M. (2025). Modeling to COVID-19 Mortality Data: Using the Neutrosophic Gompertz Inverse Rayleigh Model with Estimation, *Journal of Cultural Analysis and Social Change*, 10(4), 1766-1780. https://doi.org/10.64753/jcasc.v10i4.3076

Published: December 09, 2025

ABSTRACT

In this article, we introduce a new statistical model called the Neutrosophic inverse Gompertz Rayleigh (NGIR) distribution, which has excellent modelling to COVID-19 mortality data in the Netherlands. The model uses neutrosophic logic to address uncertainty in the data by representing parameters as time intervals (using neutrosophic logic, the direct method). The basic distribution functions were found, and several mathematical properties of the distribution were derived. Several tables illustrating the behavior of the distribution were developed based on these properties. Equations for estimating the parameters of the distribution were found using three estimation methods. The performance of NGIR was evaluated using Monte Carlo simulations of five estimation methods, and the results of these simulations were compared using several statistical measures to determine which method is best for estimation. Practical application on mortality data confirmed the model's ability to represent complex data with high degrees of uncertainty, making it a powerful tool for epidemiological analysis. The results demonstrated that NGIR outperforms other neutrosophic distributions in terms of information criteria and goodness of fit.

Keywords: Neutrosophic Logic, Inverse Rayleigh, COVID-19 Mortality, Monte Carlo Simulation, And Neutrosophic Incomplete Moments.

INTRODUCTION

Over the decades, the field of statistical distributions has undergone substantial progress. Initially, research focused on foundational distributions such as the normal and Poisson models. However, to address the growing complexity of real-world data. As challenges in data modeling became more intricate, especially in fields dealing with skewed, heavy-tailed, or highly variable data, researchers recognized the need for more adaptable probabilistic models. This increasing complexity motivated the development of new, more adaptable distribution families. Among the modern techniques proposed to address this challenge is the T-X family method, introduced in 2013 by [1], which constructs new distributions by combining a transformation function (T) with a baseline distribution (X), enabling enhanced flexibility in modeling non-standard data pattern. This method is based on functional

transformations, where new distributions are created by integrating the PDF function of the distribution, but the upper bound of the integration must be a function that satisfies the conditions of the CDF function, rather than a random variable.

Examples of these families include: Wei-G-family 2014 [2], BMO-Family 2015 [3], MKi-G-family 2020 [4], EW-G-family 2021 [5], WEE-X-2023 [6], NGOF-G-family 2023 [7], EOIW-G-family 2024 [8], HOE-Φ-family 2024 [9], and OLG family [10], all of these families, aim to provide great flexibility in data modeling.

Neutrosophic logic, proposed by Florentin Smirnić in the late 1990s, represents a generalization of fuzzy logic by incorporating a tri-component structure. Instead of evaluating propositions solely based on degrees of truth or falsehood, neutrosophic logic introduces a third dimension -indeterminacy-allowing each component: truth (T), indeterminacy (I), and falsity (F) to independently assume any value within the interval [0, 1]. This more general structure provides the ability to handle uncertain or incomplete information, especially in complex systems. In statistics the use of neutrosophic logic has enabled the construction of neutrosophic probability distributions, which take into account the uncertainty by including uncertainty in the parameters of the classical statistical model.

For example, in a neutrosophic normal distribution, the mean and standard deviation may be non-precisely defined values and are expressed as neutrosophic intervals. On one hand, modern statistical methods such as the T-X family—introduce novel distributional forms capable of capturing atypical data behavior as follows ([11], [12], [13], [14], [15], [16], [17]).

On the other hand, neutrosophic logic contributes a robust framework for representing uncertainty by transforming classical parameters and random variables into interval-based expressions. Together, these approaches open new avenues for research and application in data-driven disciplines, broadening the theoretical and practical scope of both statistics and logic

neutrosophic Gompertz-G (NGo) family introduced which has neutrosophic cumulative density function (NCDF) and neutrosophic probability density functions (NPDF), respectively, in the forms:

$$G_{NGo}(x_N) = 1 - e^{\frac{a_N}{b_N}\left(1-e^{b_N\frac{\mathcal{M}(x_N)}{1-\mathcal{M}(x_N)}}\right)} \quad (1)$$

$$g_{NGo}(x_N) = \frac{a_N m(x_N)}{\left(1-\mathcal{M}(x_N)\right)^2} e^{b_N\frac{\mathcal{M}(x_N)}{1-\mathcal{M}(x_N)}} e^{\frac{a_N}{b_N}\left(1-e^{b_N\frac{\mathcal{M}(x_N)}{1-\mathcal{M}(x_N)}}\right)} \quad (2)$$

Where $\mathcal{M}(x_N)$ and $m(x_N)$ are NCDF and NPDF for any baseline neutrosophic distribution with a neutrosophic random variable X_N, is defined as $X_N = d + kI$, where d represents the determined component and tI represents the indeterminate part. The values of kI are confined to the interval $[X_L, X_U]$, where X_L and X_U represent the lower and upper bounds of the random variable. Likewise, the values of kI fall within the range of $[I_L, I_U]$. It is crucial to note that the NGo family transforms into the classical Go family when the lower limit X_L is identical to the upper bound X_U, and Neutrosophic shape parameters a_N, and b_N, which are within the ranges $a_N \in [a_L, a_U]$, and $b_N \in [b_L, b_U]$.

The objective of this paper to introduce a novel probability distribution to model complex and uncertain statistical data like COVID-19 mortality data in neutrosophic paradigm. The aim of the study is to make the model as flexible as possible with a good fit to high variance and uncertainty of data and also to compare the performance of the model with known distributions. Additionally, the study intends to present efficient estimations of model parameters such as maximum likelihood (MLE) and application to real data to improve the accuracy of statistical analyses in epidemiological fields.

Neutrosophic Gompertz Inverse Rayleigh (NGIR) Distribution

The CDF and PDF for Inverse Rayleigh distribution, which is specified by a single parameter c. The following formulae [11] can be used to characterize these functions:

$$\mathcal{M}(x) = e^{-\frac{c}{x^2}} \quad (3)$$

$$m(x) = \frac{2c}{x^3} e^{-\frac{c}{x^2}} \quad (4)$$

The above functions (3 and 4) reflect as Neutrosophic function by replace the of the random variable X_N and parameter c with each other with the neutrosophic random variable X and neutrosophic parameter respectively

$c_N \in [c_L, c_U]$, to get a form:

$$\mathcal{M}(x_N) = e^{-\frac{c_N}{x_N^2}} \quad (5)$$

$$m(x) = \frac{2c_N}{x_N^3} e^{-\frac{c_N}{x_N^2}} \tag{6}$$

We can get the NCDF for Neutrosophic Gompertz Inverse Rayleigh (NGIR) distribution by combine the equations 5 and 1 to get a form:

$$G(x_N) = 1 - e^{\frac{a_N}{b_N}\left(\frac{b_N e^{-\frac{c_N}{x_N^2}}}{1-e^{-\frac{c_N}{x_N^2}}}\right)} \tag{7}$$

We can get the NPDF for NGIR distribution by combine the equations 5, 6 and 2 to get a form:

$$g(x_N) = \frac{2c_N a_N e^{-\frac{c_N}{x_N^2}}}{x_N^3\left(1-e^{-\frac{c_N}{x_N^2}}\right)^2} e^{\frac{b_N e^{-\frac{c_N}{x_N^2}}}{1-e^{-\frac{c_N}{x_N^2}}}} e^{\frac{a_N}{b_N}\left(\frac{b_N e^{-\frac{c_N}{x_N^2}}}{1-e^{-\frac{c_N}{x_N^2}}}\right)} \tag{8}$$

The neutrosophic survival function for NGIR can also be obtained for distribution in the formula [18], [19]:

$$S_N(x_N) = e^{\frac{a_N}{b_N}\left(\frac{b_N e^{-\frac{c_N}{x_N^2}}}{1-e^{-\frac{c_N}{x_N^2}}}\right)} \tag{9}$$

The neutrosophic hazard function for NGIR can also be obtained for distribution in the formula [20], [21]:

$$h_N(x_N) = \frac{2c_N a_N e^{-\frac{c_N}{x_N^2}}}{x_N^3\left(1-e^{-\frac{c_N}{x_N^2}}\right)^2} e^{\frac{b_N e^{-\frac{c_N}{x_N^2}}}{1-e^{-\frac{c_N}{x_N^2}}}} \tag{10}$$

Figures 1-5 present the graphs of the NGIR distribution functions for various intervals of the parameters.

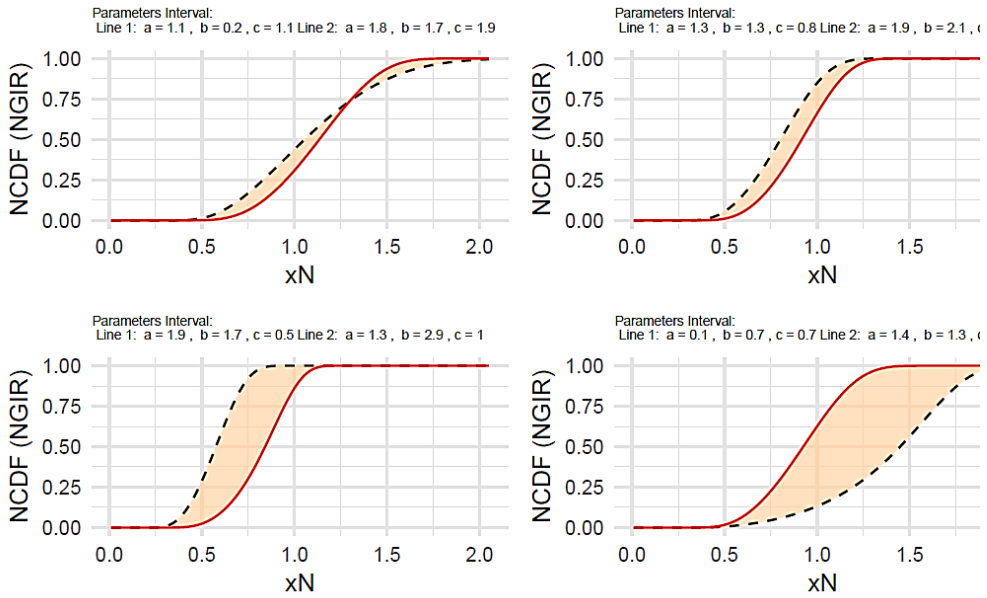

Figure 1. Plot NCDF for NGIR distribution with different interval values for parameters

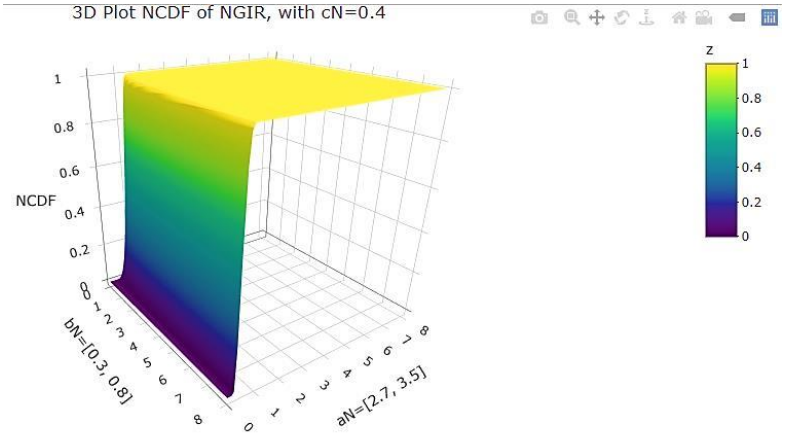

Figure 2 3D-plot NCDF for NGIR distribution

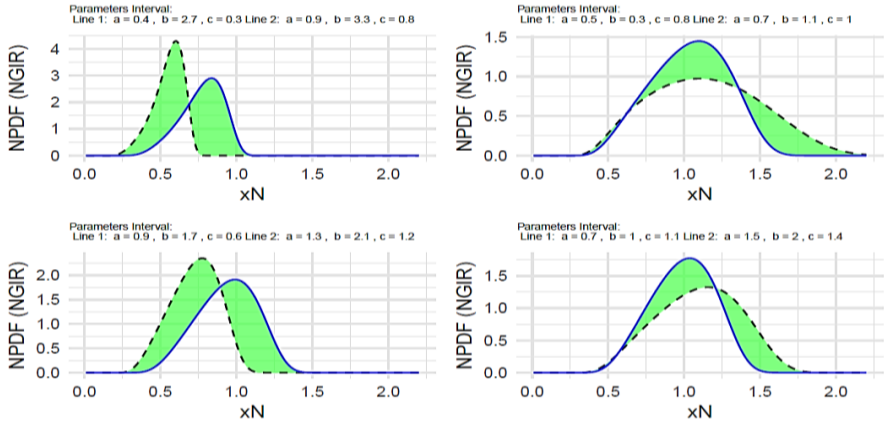

Figure 3. Plot NPDF for NGIR distribution with different interval values for parameters

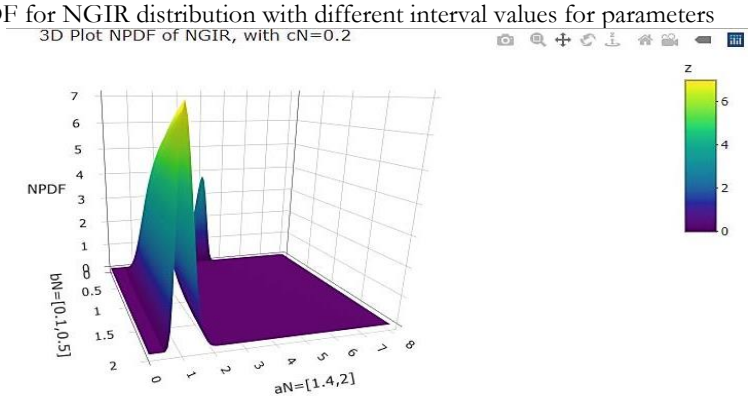

Figure 4. 3D-plot NPDF for NGIR distribution

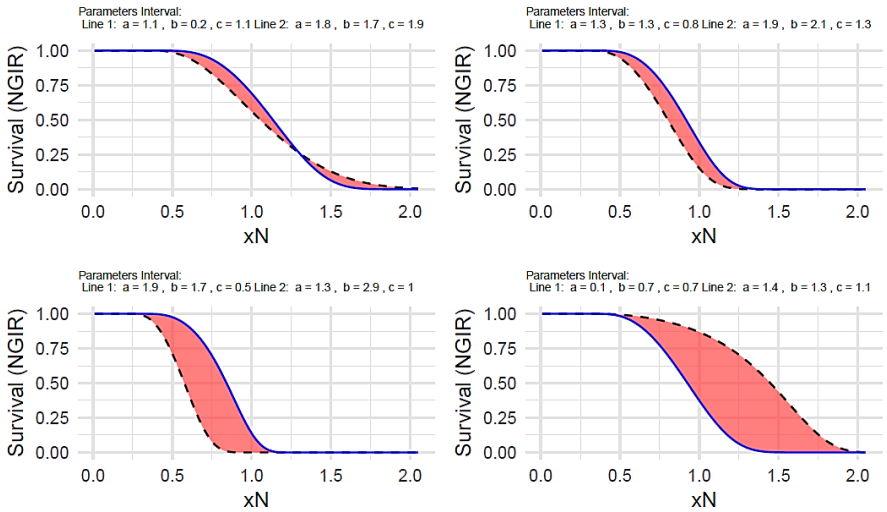

Figure 5 Plot Survival for NGIR distribution with different interval values for parameters

Figure 1:1 NCDF curve for NGIR distribution of various parameter values over ranges. It is observed that this curve represents the trend of the cumulative distribution with changes in the neutrosophic parameters which can be flexible in representing the data in the presence of uncertainty in the data.

Figure 2 presented the three-dimensional graph of the NCDF function .Which relates to how we can think about the neutrosophic random variable and its various parameters. It shows how the function changes as values of parameters vary within specified intervals. This three-dimensional curve thus underscores the very complex interplay between these variables, demonstrating how adaptable this function is to the data.

Figure 3 illustrates the NPDF curve for an NGIR distribution with distinct parameters values. In this case, we observe how the probability density distribution is affected by neutrosophic coefficients and the curves undergo certain changes regarding their shape and spread based on the parameters. This highlights the model's adaptability in capturing data that is idiosyncratic in nature, for example, extremely variant or highly skewed.

Figure 4 shows a three-dimensional view of the NPDF function. This illustration gives a clear impression of how the probability density is affected when the values of the random variable and the parameters are altered. The three-dimensional curve exposes the intricate nature of the function and illustrates how the distribution is capable of adapting to data changes while still considering uncertainty.

Figure 5 shows the neutrosophic survival function curve for an NGIR distribution with varying parameter values. The survival function defines the probability of a random variable staying above a certain value, and this curve shows the changes in this probability due to the changes in the neutrosophic coefficients. The curves show different patterns regarding the behavior of the survival function which demonstrates the capability of the model to describe data with large degrees of uncertainty.

Properties for NGIR Distribution

Mathematical Representation

Proving the mathematical properties of the NGIR distribution poses problems in dealing with its more basic distribution functions. Hence, the NCDF and NPDF functions are simplified through the use of exponential function expansion and scalar expansion [22], [23] as follows

$$G(x_N) = 1 - \Psi e^{-b_N(k_N+s_N)x_N^{-2}} \quad (11)$$

$$g(x_N) = \gamma 2\mathrm{b_N} x_N^{-3} e^{-b_N(t_N+v_N+1)x_N^{-2}} \quad (12)$$

The functions G^{δ_N} and g^{β_N} are also needed to prove some properties. Therefore, these functions are simplified in the same manner, as follows:

$$G^{\delta_N}(x_N) = Te^{-b_N(z_N+p_N)x_N^{-2}} \quad (13)$$

$$g^{\beta_N}(x_N) = 2E\mathrm{b_N} x_N^{-3} e^{-b_N(m_N+\varepsilon_N+\beta_N)x_N^{-2}} \quad (14)$$

where $\Psi = \sum_{i_N=j_N=k_N=s_N=0}^{\infty} \frac{(-1)^{j_N}\Gamma(k_N,s_N)}{i_N!k_N!s_N!\Gamma(k_N)} a_N^{i_N} b_N^{k_N-i_N} j_N^{k_N}$,

$\gamma = \sum_{i_N=j_N=t_N=0}^{\infty} \frac{(-1)^{j_N}\Gamma(t_N+2,v_N)}{i_N!t_N!v_N!\Gamma(t_N+2)} \binom{i_N}{j_N} a_N^{i_N+1} b_N^{-i_N} b_N^{t_N} (j_N+1)^{t_N}$,

$T = \sum_{l_N=w_N=r_N=z_N=p_N=0}^{\infty} \frac{(-1)^{l_N+w_N+r_N+z_N}\Gamma(z_N,p_N)}{w_N!z_N!p_N!\Gamma(z_N)} \binom{\delta_N}{l_N} \binom{w_N}{r_N} a_N^{w_N} l_N^{w_N} b_N^{z_N-w_N} r_N^{z_N}$, and

$E = \sum_{d_N=q_N=m_N=\varepsilon_N=0}^{\infty} \frac{(-1)^{q_N}\Gamma(2\beta_N+m_N,\varepsilon_N)}{d_N!m_N!b_N^{d_N}\varepsilon_N!\Gamma(2\beta_N+m_N)} \binom{d_N}{q_N} a_N^{d_N+\beta_N} \beta_N^{d_N} b_N^{m_N} (\beta_N+q_N)^{m_N}$.

The Neutrosophic Moments

Let X_N be any neutrosophic random variable, then the n^{th} neutrosophic moments for any neutrosophic can expressing as form [24]:

$$\mu_n' = E(x_N^n) = \int_0^{\infty} x_N^n \, g(x_N) dx_N$$

Substitution equation 12 in above equation to get the n^{th} neutrosophic moments for NGIR distribution by form:

$$\mu_n' = \gamma \int_0^{\infty} x_N^n \, 2\mathrm{b_N} x_N^{-3} e^{-b_N(t_N+v_N+1)x_N^{-2}} dx_N$$

By solving the above integral, we obtain the neutrosophic moment function for the distribution in the form:

$$\mu_n' = \gamma [b_N(t_N+v_N+1)]^{\frac{n}{2}-1} \Gamma\left(1-\frac{n}{2}\right) \quad (15)$$

In order to identify the nature of the distribution in finding moments, as well as the values of variance, skewness, and kurtosis, Table 1 is prepared, as follows:

Table.1 some intervals of moments for NGIR distribution

a_N	b_N	c_N	$\grave{\mu}_{1_N}$	$\grave{\mu}_{2_N}$	$\grave{\mu}_{3_N}$	$\grave{\mu}_{4_N}$	σ_N^2	S_N	K_N
[0.6,1.6]	[0.3,1.3]	[0.1,1.1]	[0.384902, 0.53043]	[0.162865, 0.430025]	[0.074459, 0.357749]	[0.03625, 0.30407]	[0.014715, 0.148669]	[1.132859, 1.268638]	[1.366638, 1.644316]
		[0.2,1.2]	[0.541043, 0.480837]	[0.322313, 0.394314]	[0.20705, 0.331147]	[0.141304, 0.283666]	[0.029585, 0.163109]	[1.13151, 1.33739]	[1.360186, 1.824414]
	[0.5,1.5]	[0.3,1.3]	[0.61549, 0.446578]	[0.417485, 0.370406]	[0.300466, 0.313993]	[0.226594, 0.271063]	[0.038657, 0.170974]	[1.11387, 1.392849]	[1.300068, 1.97567]
		[0.4,1.4]	[0.606161, 0.401088]	[0.445274, 0.335366]	[0.343758, 0.286165]	[0.275817, 0.248377]	[0.077842, 0.174494]	[1.156944, 1.473457]	[1.391128, 2.208377]
[0.9,1.9]	[0.7,1.7]	[0.5,1.5]	[0.634303, 0.414714]	[0.464307, 0.348283]	[0.355943, 0.298165]	[0.283149, 0.259431]	[0.061967, 0.176295]	[1.12505, 1.450636]	[1.31342, 2.13874]
		[0.6,1.6]	[0.595121, 0.373748]	[0.452961, 0.316033]	[0.35893, 0.272083]	[0.293708, 0.237843]	[0.098792, 0.176345]	[1.177385, 1.53145]	[1.431512, 2.381368]
	[0.9,1.9]	[0.7,1.7]	[0.56983, 0.343111]	[0.445838, 0.292244]	[0.361208, 0.25313]	[0.300932, 0.222399]	[0.121132, 0.174519]	[1.213365, 1.602233]	[1.513958, 2.60401]
		[0.8,1.8]	[0.462908, 0.292924]	0.37013, 0.250921]	[0.305314, 0.218365]	[0.258225, 0.192611]	[0.155846, 0.165116]	[1.35586, 1.737313]	[1.884902, 3.059204]

Results indicate that the mean $\grave{\mu}_{1_N}$N appears to exhibit a gradual contraction with increasing the parameter value, particularly as c_N_N transitions from the greatest to the smallest interval where the mean decreases. This suggests that the distribution is pulled toward lower values as the parameters increase and may represent the nature of an NGIR distribution in which large parameter values tend to shift the distribution in the left tail. There is, however, a significant widening of the variance with increasing parameters which suggests a moderate to strong level of dispersion in the data. This behavior can be explained by the neutrosophic nature of the distribution which allows for greater uncertainty in the data due to the wide range of parameter values, resulting in higher variance. Looking at the shape of the distribution, the skewness coefficient shows positive values for all groups indicating that the distribution is always right-skewed. This implies that the distribution possibly has thicker tails compared to a normal distribution

The Neutrosophic Moment Generating Function

The Neutrosophic Moment Generating Function (NMGF) for NGIR distribution, from neutrosophic moment function and exponential expansion can be get a form [25]:

$$M_x(t) = E(e^{tx}) = \int_0^{\infty} e^{tx} g(x_N) dx$$

$$M_x(t) = \sum_{r=0}^{\infty} \frac{t^r}{r!} \left[-\gamma b_N^{\frac{n}{2}} \left(b_N (t_N + v_N + 1) \right)^{\frac{n-2}{2}} \Gamma\left(1 - \frac{n}{2}\right) \right] \quad (16)$$

The Neutrosophic Characteristic Function

The Neutrosophic Characteristic function (NCF) for NGIR distribution, from neutrosophic moment function and exponential expansion can be get a form [25]:

$$Q_x(t) = E\left(e^{itx}\right) = \int_0^{\infty} e^{itx} g(x_N) dx$$

$$Q_x(t) = \sum_{v=0}^{\infty} \frac{(it)^v}{v!} \left[-\gamma b_N^{\frac{n}{2}} \left(b_N(t_N + v_N + 1)\right)^{\frac{n-2}{2}} \Gamma\left(1 - \frac{n}{2}\right)\right] \quad (17)$$

The Neutrosophic Incomplete Moments

Let X_N be any neutrosophic random variable, then the n^{th} neutrosophic Incomplete moments for any neutrosophic can expressing as form [24]:

$$M_n(y_N) = \int_0^{y_N} x_N^n \, g(x_N) dx_N$$

Substitution equation 12 in above equation to get the n^{th} neutrosophic Incomplete moments for NGIR distribution by form:

$$M_n(y_N) = \gamma \int_0^{y_N} x_N^n \, 2\mathrm{b_N} x_N^{-3} e^{-b_N(t_N + v_N + 1)x_N^{-2}} dx_N$$

By solving the above integral, we obtain the neutrosophic moment function for the distribution in the form:

$$M_n(y_N) = \gamma [b_N(t_N + v_N + 1)]^{\frac{n}{2}-1} \Gamma\left(\left(1 - \frac{n}{2}\right), \frac{b_N(t_N + v_N + 1)}{y_N^2}\right) \quad (18)$$

Neutrosophic Probability Weighted Moments

We may calculate the Neutrosophic probabilistic weighted moments of the NGIR distribution by applying the following equation [26]:

$$\tau_{k,\delta_N} = E\left(x_N^k G^{\delta_N}(x_N)\right) = \int_{-\infty}^{\infty} x_N^k g(x_N) G^{\delta_N}(x_N) dx_N$$

By substitute equation 12 and 13 in above equation to get a formula:

$$\tau_{k,\delta_N} = \gamma T \int_0^{\infty} x_N^k 2\mathrm{b_N} x_N^{-3} e^{-b_N(t_N + v_N + z_N + p_N + 1)x_N^{-2}} dx$$

Then, integrate the preceding equation to obtain the final formula:

$$\tau_{k,\delta_N} = \gamma T [b_N \theta]^{\frac{k}{2}-1} \Gamma\left(1 - \frac{k}{2}\right), \theta = t_N + v_N + z_N + p_N + 1 \quad (19)$$

where $k = 0 \Longrightarrow \tau_{0,\delta_N} = \frac{\gamma T}{b_N \theta}$

Neutrosophic Quantile Function

Neutrosophic quantile function is the inverse of the NCDF. Mathematically, if $G(x_N)$ is the NCDF of a Neutrosophic random variable, then the Neutrosophic quantile function $Q_N(p)$ is defined by the relationship:

$$Q_N(q) = G^{-1}(x_N) = inf\{x_N \in \mathbb{R}^2 : G(x_N) > q\} \quad (20)$$

where $q \in [0,1]$ represents the desired probability. In short, the quantile function returns the value x_N for which $P(X_N \leq x_N) = q$, put:

$$q = 1 - e^{\frac{a_N}{b_N}\left(1 - e^{b_N \frac{e^{-\frac{c_N}{x_N^2}}}{1 - e^{-\frac{c_N}{x_N^2}}}}\right)} \quad (21)$$

Then we get a final form:

$$x_N = \sqrt{\frac{-c_N}{\log\left[\frac{\frac{1}{b_N}\log\pi}{\left(1 + \frac{1}{b_N}\log\pi\right)}\right]}}, \pi = 1 - \frac{b_N}{a_N}\log(1 - q) \quad (22)$$

The following table shows the values of the Neutrosophic quantile function with different parameter intervals.

Table 2: Neutrosophic Quantile function for NGIR distribution

q	(a_N, b_N, c_N)				
	[0.5, 1.5],	**[0.4, 1.4],**	**[0.7,1.7],**	**[0.6,1.6],**	**[0.5,1.5],**

	[0.7, 1.7] [0.9, 1.9]	**[0.7, 1.7] [0.2, 1.2]**	**[0.8.1,8] [0.5,1.5]**	**[0.4,1.4] [0.2,1.2]**	**[0.9,1.9] [1,2]**
0.1	[0.7058782, 0 .8271578]	[0.3496091,0.664 6916]	[0.4898231,0. 7202573]	[0.3218739,0.651 6492]	[0.7408879, 0.8 477526]
0.2	[0.8405100, 0 .9412064]	[0.4190495, 0.75 76202]	[0.5756444,0. 8165176]	[0.3838953,0.741 8687]	[0.8774080, 0.9 632432]
0.3	[0.9469469, 1 .0294006]	[0.4731563, 0.82 93347]	[0.6439112,0. 8909101]	[0.4351759,0.812 6293]	[0.9829988, 1.0 518574]
0.4	[1.0401777, 1 .1063648]	[0.5198557, 0.89 17266]	[0.7043404,0. 9558839]	[0.4820498,0.875 2755]	[1.0738395, 1.1 285727]
0.5	[1.1266220, 1 .1779766]	[0.5625759, 0.94 96361]	[0.7609793,1. 0164873]	[0.5273073,0.934 3506]	[1.1568185, 1.1 995148]
0.6	[1.2105646, 1 .2479888]	[0.6035596, 1.00 60239]	[0.8166026,1. 0758620]	[0.5729722,0.992 9062]	[1.2362943, 1.2 684365]
0.7	[1.2962159, 1 .3200510]	[0.6449170, 1.06 38906]	[0.8739528,1. 1371230]	[0.6213306,1.053 9394]	[1.3164778, 1.3 389694]
0.8	[1.3899263, 1 .3996793]	[0.6896758, 1.12 76801]	[0.9373680,1. 2050287]	[0.6761733,1.122 2641]	[1.4032822, 1.4 165051]
0.9	[1.5075462, 1 .5008758]	[0.7453438, 1.20 84484]	[1.0178423,1. 2915840]	[0.7477535,1.210 3214]	[1.5111508, 1.5 144485]

Based on the conclusions from the table, it can be noted that the quantile function exhibits different behavior primarily based on the value of the parameter and the probability q As shown in the table above, when q equals 0.1, the quantile value for the first set of parameters is [(0.5,1.5),(0.7,1.7),(0.9,1.9)]=[0.7058782,0.8271578]. The relatively wide range indicates a high degree of uncertainty which is consistent with the nature of neutrosophic data that deals with ambiguity and indeterminacy. Additionally we also note that for q value equal to 0.5, which is 50%, it can be seen that the quantile value is increasing for all sets of parameters which is more pronounced in lower ranges of q, even if that means lower quantile values.

In general all the results from the table suggest that the neutrosophic quantile function for the NGIR distribution does indeed cover wide ranges of probability while accounting for uncertainty pertaining to the parameters and yielding results with high value for complex data where, uncertainty and imprecision abound. It is also noted that the results are highly sensitive towards choosing the right intervals for declaring the range of the quantile values.

Neutrosophic Rényi Entropy

Neutrosophic Rényi Entropy for NGIR distribution obtained by form [27]:

$$I_R(\beta_N) = \frac{1}{1-\beta_N} log \int_0^{\infty} g(x_N)^{\beta_N} dx_N$$

Substituting equation 14 into the equation above, we get:

$$I_R(\beta_N) = \frac{1}{1-\beta_N} log \int_0^{\infty} 2E\mathrm{b_N} x_N^{-3} e^{-b_N(m_N+\varepsilon_N+\beta_N)x_N^{-2}} dx_N \quad (23)$$

By solving the above integral, we obtain the neutrosophic moment function for the distribution in the form:

$$I_R(\beta_N) = \frac{1}{1-\beta_N} log \left[\frac{E}{(m_N+\varepsilon_N+\beta_N)}\right] \quad (24)$$

Estimation Parameters for NGIR Distribution

Maximum Likelihood Estimation - MLE

Maximum likelihood estimation is defined as a method in which the values of the unknown parameters of a statistical model are determined by maximizing the likelihood function, which represents the probability of observing the given data under the proposed model. Mathematically, if we have a sample of data $X_N = (x_{N1}, x_{N2}, \ldots, x_{Nn})$ and a probability distribution $f(x_N|\theta_N)$ where θ_N are unknown parameters, the likelihood function is written as [28], [29]:

$$L(\Theta_N, x_N) = \prod_{i=1}^{n} g(x_N)$$

$$L(\Theta_N, x_N) = \prod_{i=1}^{n} \frac{a_N 2\mathrm{b}_\mathrm{N} x_N^{-3} e^{-b_N x_N^{-2}}}{\left(1 - e^{-b_N x_N^{-2}}\right)^2} e^{b_N \frac{e^{-b_N x_N^{-2}}}{1-e^{-b_N x_N^{-2}}}} e^{\frac{a_N}{b_N}\left(1-e^{b_N \frac{e^{-b_N x_N^{-2}}}{1-e^{-b_N x_N^{-2}}}}\right)}$$

We compute the log- likelihood:

$$L = n \log a_N + n \log(2\mathrm{b}_\mathrm{N}) - 3\sum_{i=1}^{n} \log x_{\mathrm{iN}} - \sum_{i=1}^{n} b_N x_{iN}^{-2} + b_N \sum_{i=1}^{n} \frac{e^{-b_N x_{iN}^{-2}}}{1 - e^{-b_N x_{iN}^{-2}}}$$
$$-2\sum_{i=1}^{n} \log\left(1 - e^{-b_N x_{iN}^{-2}}\right) + \frac{a_N}{b_N} \sum_{i=1}^{n} 1 - e^{b_N \frac{e^{-b_N x_{iN}^{-2}}}{1-e^{-b_N x_{iN}^{-2}}}} \quad (25)$$

Ordinary Least Squares - LSE

The ordinary least squares method is used to estimate the coefficients by minimizing the sum of squared differences between the observed and predicted values. The equation for the method is given by the formula [30], [31]:

$$\varphi(\theta_N) = \sum_{i=1}^{m} \left[G(x_{Ni}) - \frac{i}{n+1}\right]^2$$

$$\varphi(\theta_N) = \sum_{i=1}^{n} \left[1 - e^{\frac{a_N}{b_N}\left(1-e^{b_N \frac{e^{-b_N x_N^{-2}}}{1-e^{-b_N x_N^{-2}}}}\right)} - \frac{i}{n+1}\right]^2 \quad (26)$$

Weighted Least Squares - WLS

The ordinary least squares method is used to estimate the coefficients by minimizing the sum of squared differences between the observed and predicted values. The equation for the method is given by the formula [25], [32]:

$$W(\theta_N) = \sum_{i=1}^{n} W_i \left[G(x_{Ni}) - \frac{i}{n+1}\right]^2$$

$$W(\theta_N) = \sum_{i=1}^{n} W_i \left[1 - e^{\frac{a_N}{b_N}\left(1-e^{b_N \frac{e^{-b_N x_N^{-2}}}{1-e^{-b_N x_N^{-2}}}}\right)} - \frac{i}{n+1}\right]^2 \quad (27)$$

Simulation

Estimating complex distributions with random sample methodologies employs Monte Carlo algorithms. For this study, these algorithms were utilized to assess how accurately five estimators (MLE, LSE, WLSE, ADE, RTADE) estimate the neutrosophic (fuzzy bounds, not sharply defined) parameter NGIR distribution across sample sizes N = 50, 100, 150, 200, … up to 1000. The outcomes were evaluated through mean square error (MSE) and root mean square error (RMSE) alongside bias calculations [33], [34]. The simulation results demonstrate estimating parameters a_N , b_N, and c_N for compound neutrosophic intervals were the most accurate at sample sizes N = 50, 100, 150, and 200. Those sample sizes are presented in Table 3 along with the beyond bound sample ranges.

Table 3: Monte Carlo simulations conducted for NGIR distribution

a_N = [3 , 4], b_N = [1.5 , 1.9], c_N = [4 , 5]							
N	**Est.**	**Ess. Par.**	**MLE**	**LSE**	**WLSE**	**ADE**	**RTADE**
		$\widehat{a_N}$	[3.9917893, 5.143415]	[4.738623, 5.707372]	[4.328175, 5.373994]	[4.439933, 5.586339]	[13.66783, 16.72482]
		$\widehat{b_N}$	[1.48804362, 1.96946326]	[0.6342964, 0.9787356]	[0.9317916, 1.2897713]	[1.0576053, 1.4499344]	[-24.13027, -19.71914]
50	**Mean**	$\widehat{c_N}$	[4.1572593, 5.1066804]	[4.03414323, 4.8707255]	[4.03280694, 4.90882874]	[4.1392705, 5.04556834]	[0.4770653, 0.6105288]

		$\widehat{a_N}$	[11.7349440, 20.590970]	[36.820765, 42.360068]	[22.351758, 31.253529]	[21.257898, 32.830854]	[156.29793, 213.87533]
		$\widehat{b_N}$	[0.91061798, 1.61547104]	[5.3305295, 5.9705607]	[2.4585748, 3.6179930	[2.1103319, 3.1313901]	[538.68577, 785.70433]
	MSE	$\widehat{c_N}$	[1.3654623, 1.7436138]	[2.28251487, 2.9297338]	[1.87948845, 2.39856760]	[1.7628712, 2.21794708]	[12.4434642, 19.3260501]
		$\widehat{a_N}$	[3.4256305, 4.537727]	[6.068012, 6.508461]	[4.727765, 5.590486]	[4.610629, 5.729821]	[12.50192, 14. 62448]
		$\widehat{b_N}$	[0.95426306, 1.27101182]	[2.3087939, 2.4434731]	[1.5679843, 1.9021022]	[1.4526982, 1.7695734]	[23.20961, 28.03042]
	RMSE	$\widehat{c_N}$	[1.1685300, 1.3204597]	[1.51079941, 1.7116465]	[1.37094436, 1.54873097]	[1.3277316, 1.48927737]	[3.5275295, 4.3961404]
		$\widehat{a_N}$	[0.9917893, 1.143415]	[1.707372, 1.738623]	[1.328175, 1.373994]	[1.439933, 1.586339]	[10.66783, 12. 72482]
		$\widehat{b_N}$	[0.01195638, 0.06946326]	[0.8657036, 0.9212644]	[0.5682084, 0.6102287]	[0.4423947, 0.4500656]	[21.21914, 26.03027]
	Bias	$\widehat{c_N}$	[0.1066804, 0.1572593]	[0.1292745, 0.03414323]	[0.03280694, 0.09117126]	[0.04556834,0.13 92705]	[3.5229347, 4.3894712]
		$\widehat{a_N}$	[3.3371217, 4.5925015]	[3.5789559, 4.8551058]	[3.4446231, 4.7344332]	[3.5099832, 4.8252873]	[14.01895, 17. 32226]
		$\widehat{b_N}$	[1.51818277, 1.91500837]	[1.1506284, 1.4378564]	[1.2995323, 1.608203]	[1.3361653, 1.6528578]	[-24.99249, - 20.22584]
	Mean	$\widehat{c_N}$	[4.02112953, 5.06446168]	[3.92451635, 4.90217145]	[3.96565557, 4.97987068]	[4.01959377, 5.04276528]	[0.4287158, 0.5636387]
		$\widehat{a_N}$	[3.6125607, 7.3270065]	[8.4291834, 16.4321908]	[5.6892027, 11.5266142]	[5.4656765, 10.9631504]	[150.43933, 207 .42677]
		$\widehat{b_N}$	[0.35229733, 0.70861960]	[1.2640953, 2.1786850]	[0.6789265, 1.249400]	[0.6277198, 1.1773632]	[532.42010, 785.54847]
	MSE	$\widehat{c_N}$	[0.62821559, 0.91991102]	[1.15557313, 1.68417783]	[0.82940438, 1.25063673]	[0.76376007, 1.17656029]	[12.7704225, 19.7189451]
		$\widehat{a_N}$	[1.9006738, 2.7068444]	[2.9033056, 4.0536639]	[2.3852050, 3.3950868]	[2.3378786, 3.3110648]	[12.26537, 14. 40232]
		$\widehat{b_N}$	[0.59354640, 0.84179546]	[1.1243199, 1.4760369]	[0.8239700, 1.117766]	[0.7922877, 1.0850637]	[23.07423, 28.02764]
	RMSE	$\widehat{c_N}$	[0.79260052, 0.95911992]	[1.07497588, 1.29775877]	[1.117766, 1.11831871]	[0.87393367, 1.08469364]	[3.5735728, 4.4406019]
		$\widehat{a_N}$	[0.3371217, 0.5925015]	[0.5789559, 0.8551058]	[0.4446231, 0.7344332]	[0.5099832, 0.8252873]	[11.01895, 13. 32226]
		$\widehat{b_N}$	[0.01818277, 0.01500837]	[0.3493716, 0.4621436]	[0.2004677, 0.291797]	[0.1638347, 0.2471422]	[21.72584, 26.89249]
100	**Bias**	$\widehat{c_N}$	[0.02112953, 0.06446168]	[0.07548365, 0.09782855]	[0.03434443, 0.03434443]	[0.01959377, 0.04276528]	[3.5712842, 4.4363613]
		$\widehat{a_N}$	[3.2330815, 4.3825372]	[3.5090559, 4.522526]	[3.3452902, 4.4250597]	[3.3715099, 4.4821055]	[14.25986, 18. 02245]
		$\widehat{b_N}$	[1.51730916, 1.92175581]	[1.2300223, 1.6148214]	[1.3665041, 1.7516043]	[1.3858205, 1.7765209]	[-20.57370, - 26.00290]
	Mean	$\widehat{c_N}$	[4.02293709, 5.05377072]	[3.992741011, 4.92003202]	[4.005035421, 4.98370275]	[4.02867704, 5.02388901]	[0.4154863, 0.5407019]
		$\widehat{a_N}$	[2.2530450, 4.2097783]	[5.7130047, 9.617191]	[3.4001204, 6.2313956]	[3.2735087, 5.9360876]	[144.75355, 205 .89467]
		$\widehat{b_N}$	[0.22752012, 0.38801520]	[0.7809542, 1.2037000]	[0.3974947, 0.6700489]	[0.3939752, 0.6270253]	[524.65840, 797.86398]
	MSE	$\widehat{c_N}$	[0.41647403, 0.61431219]	[0.802778843, 1.20738948]	[0.557719932, 0.83127037]	[0.52553410, 0.78372013]	[12.8601771, 19.9116158]
		$\widehat{a_N}$	[1.5010147, 2.0517744]	[2.3901893, 3.101160]	[1.8439415, 2.4962764]	[1.8092840, 2.4364087]	[12.03136, 14. 34903]
		$\widehat{b_N}$	[0.47699069, 0.62290866]	[0.8837161, 1.0971326]	[0.6304718, 0.8185651]	[0.6276745, 0.7918493]	[22.90542, 28.24649]
	RMSE	$\widehat{c_N}$	[0.64534799, 0.78378070]	[0.895979265, 1.09881276]	[0.746806489, 0.91174030]	[0.72493731, 0.88527969]	[3.5861089, 4.4622434]
		$\widehat{a_N}$	[0.2330815, 0.3825372]	[0.5090559, 0.522526]	[0.3452902, 0.4250597]	[0.3715099, 0.4821055]	[11.25986, 14. 02245]
		$\widehat{b_N}$	[0.01730916, 0.02175581]	[0.2699777, 0.2851786]	[0.1334959, 0.1483957]	[0.1141795, 0.1234791]	[22.07370, 27.90290]
150	**Bias**	$\widehat{c_N}$	[0.02293709, 0.05377072]	[0.007258989, 0.07996798]	[0.005035421, 0.01629725]	[0.02867704, 0.02388901]	[3.5845137, 4.4592981]
		$\widehat{a_N}$	[3.178766, 4.3341579]	[3.2757924, 4.5264064]	[3.1961086, 4.4394571]	[3.2328265, 4.469106]	[14.23228, 14.23 228]
		$\widehat{b_N}$	[1.5009392485, 1.90880226]	[1.3323917, 1.6457617]	[1.41553979, 1.7529745]	[1.42216229, 1.7729688]	[-20.53375, - 26.14192]
	Mean	$\widehat{c_N}$	[4.01770083, 5.0534642]	[3.95167704, 4.98833161]	[3.97905509, 5.02742585]	[4.003741712, 5.05069556]	[0.40112790.530 2202]
		$\widehat{a_N}$	[1.469628, 3.0763090]	[3.5873899, 7.0042411]	[2.1473035, 4.6317177]	[2.0778749, 4.417308]	[129.94555, 20 7.95695]
200	**MSE**	$\widehat{b_N}$	[0.1430850599, 0.28597103]	[0.4365696,0.8751362]	[0.22788066, 0.4815695]	[0.22701091, 0.4589775]	[493.35856, 804.27716]

		$\widehat{c_N}$	[0.29702909, 0.4556755]	[0.58842419, 0.87715491]	[0.39471441, 0.61731889]	[0.373341717, 0.58668344]	[12.9606399, 20.0024963]
	RMSE	$\widehat{a_N}$	[1.212282, 1.7539410]	[1.8940406, 2.6465527]	[1.4653681, 2.1521426]	[1.4414836, 2.101739]	[11.39937, 14. 42071]
		$\widehat{b_N}$	[0.3782658588, 0.53476259]	[0.6607341, 0.9354871]	[0.47736848, 0.6939521]	[0.47645662, 0.6774788]	[22.21168, 28.35978]
		$\widehat{c_N}$	[0.54500375, 0.6750374]	[0.76708813, 0.93656549]	[0.62826301, 0.78569644]	[0.611016953, 0.76595264]	[3.6000889, 4.4724150]
	Bias	$\widehat{a_N}$	[0.178766, 0.3341579]	[0.2757924, 0.5264064]	[0.1961086, 0.4394571]	[0.2328265, 0.469106]	[11.23228, 14. 11899]
		$\widehat{b_N}$	[0.0009392485, 0.00880226]	[0.1676083, 0.2542383]	[0.08446021, 0.1470255]	[0.07783771, 0.1270312]	[22.03375, 28.04192]
		$\widehat{c_N}$	[0.01770083, 0.0534642]	[0.04832296, 0.01166839]	[0.02094491, 0.02742585]	[0.003741712, 0.05069556]	[3.5988721, 4.4697798]

From table 3:

- MLE: The MLE estimations exhibited the lowest level of bias (Bias) and the lowest mean squared error (MSE) for the majority of parameters, particularly as the sample size increased (N = 200). In case of a sample size of 200, the MLE had lower bias than the LSE for all parameters and lower MSE. This is the advantage that MLE have received, as it can take full advantage of distribution probability characteristics, therefore, being capable of performance well enough when handling complex data.
- WLSE: It ranked second best, better than LSE but not as best as MLE. Improving with more samples is what we saw. This is because WLSE can fix heteroscedasticity since it gives different weights to observations; hence, it reduces outlier impacts.
- LSE: LSE performed less efficiently compared to the earlier two methods; it recorded higher values for both bias and mean square error. The weakness of this method is attributed to the strict assumptions of LSE, like homogeneity of variance and correlation-free errors, which may not hold in real data.ADE: ADE recorded intermediate values for bias (BIAS) and mean square error (MSE) compared to MLE and WLSE, but outperformed LSE in some cases. ADE showed improvement with increasing sample size, but this improvement was less pronounced compared to MLE
- RTADE: RTADE executed the worst among all methods, with a very high bias. This poor performance is due to RTADE focusing on the right tail of the distribution; it is highly sensitive to outliers in neutrosophic data, where wide parameter intervals are additional sources of instability.
- While WLSW and ADE perform okay in some situations, MLE is still the best method for estimating parameters of the NGIR distribution because of its high accuracy and stability. RTADE seems inappropriate for this model due to its huge bias and skewing over wide intervals. WLSW and ADE should be used only as supplementary means of checking results; they cannot replace MLE in actual applications.

Application

Given the complexities associated with analyzing epidemiological data, especially in the context of the COVID-19 pandemic [35], there is a need for flexible probability distributions capable of representing the high uncertainty and variability in the data. The NGIR distribution provides an advanced mathematical framework for modeling such data, incorporating the concept of interval-valued parameters to capture the inherent ambiguity in the data. In this section, the performance of the NGIR distribution is evaluated compared to six other neutrosophic distributions, e.g., Neutrosophic Odd Lomax Inverse Rayleigh (NOLIR), neurosophic Kumaraswamy (NKuIR), Neutrosophic Exponeted Generalized Inverse Rayleigh (NEGIR), neutrophilic log-gamma Inverse Rayleigh (NLGIR), neutrophilic beta Inverse Rayleigh (NBIR), and neutrophilic Inverse Rayleigh (NIR), using Dutch COVID-19 mortality data. The comparison relies on integrated informatics (AIC [41], CAIC [36], BIC [37] , HQIC [38]) and statistical criteria (p-value, Anderson-Darling (A) [39], Cramér-von Mises (W) [4], and Kolmogorov-Smirnov (KS) [40], [41]) to identify the best model and statistical measures.

The following table presents a statistical summary of a variable (Var) measured in a sample of 30 observations (N = 30), along with some statistical values for the data used. The data are presented in the form of neutrosophic intervals (interval-valued), meaning that each statistic has a lower and an upper limit.

Var	N	Mean	SD	Median	Trimmed	Mad	Min	Max	Range	SK	KU	Se
1	**30**	**[6.14, 6.36]**	**[3.51, 3.56]**	**[5.37, 5.64]**	**[5.79 , 6]**	**[2.72, 2.85]**	**[1.27 , 1.34]**	**[14.92,15.66]**	**[13.64,14.33]**	**[0.8, 0.82]**	**[-0.18,0.3]**	**[0.64,0.65]**

Tables 4 to 6 show the results of comparing the NGIR distribution with other distributions.

Table 4. results of the criteria for the distributions

Dist.	-log	AIC	CAIC	BIC	HQIC
NGIR	[76.3853, 76.97917]	[158.7706, 159.9583]	[159.6937, 160.8814]	[162.9742, 164.1619]	[160.1154, 161.3031]
NOLIR	[83.4867, 84.64634]	[172.9734, 175.2927]	[173.8965, 176.2158]	[177.177, 179.4963]	[174.3182, 176.6375]
NKuIR	[82.26124, 83.20338]	[170.5225, 172.4068]	[171.4456, 173.3298]	[174.7261, 176.6104]	[171.8672, 173.7515]
NEGIR	[81.0586, 82.0396]	[168.1172, 170.0792]	[169.0403, 171.0023]	[172.3208, 174.2828]	[169.462, 171.424]
NLGamIR	[78.11411, 78.84877]	[162.2282, 163.6975]	[163.1513, 164.6206]	[166.4318, 167.9011]	[163.573, 165.0423]
NBeIR	[82.04871, 82.99777]	[170.0974, 171.9955]	[171.0205, 172.9186]	[174.301, 176.1991]	[171.4422, 173.3403]
NIR	[83.11783, 83.9568]	[168.2357, 169.9136]	[168.3785, 170.0565]	[169.6369, 171.3148]	[168.6839, 170.3618]

Table 5. value of the statistical measures

Dist.	W	A	K-S	p-value
NGIR	[0.0268702, 0.02770035]	[0.1855461, 0.1890523]	[0.08034257,0.08649474]	[0.9639576, 0.9816981]
NOLIR	[0.2297134, 0.2534004]	[1.445338, 1.567715]	[0.1907744, 0.1914555]	[0.1945301, 0.1977047]
NKuIR	[0.1927844, 0.2104938]	[1.237822,, 1.326984]	[0.1917165 , 0.1928729]	[0.1880491, 0.1933235]
NEGIR	[0.1466052, 0.1657331]	[0.9725824, 1.070791]	[0.1546121, 0.1587126]	[0.3950125, 0.4270969]
NLGamIR	[9.713265, 9.742436]	[59.80061, 59.85859]	[0.9933995, 0.9937315]	[1.221245e-15,1.221245e-15]
NBeIR	[0.1857669, 0.2037795]	[1.197997, 1.288988]	[0.1837796, 0.1851674]	[0.2253741, 0.2326529]
NIR	[0.1875187, 0.2053168]	[1.208044, 1.297796]	[0.2179057, 0.2181093]	[0.0985182,0.09906559]

Table 6. Estimator value interval for parameters by MLE

Dist.	$\hat{a}_N$	$\hat{b}_N$	$\hat{c}_N$
NGIR	[0.063694659, 0.060528236]	[0.006384761, 0.006563764]	[2.5641639722.898459181]
NOLIR	[26.420065, 46.810342]	[17.567029, 29.835744]	[5.055747, 5.739065]
NKuIR	[3.0874136, 3.2610057]	[0.7395029, 0.7521805]	[3.0874136, 3.2610057]
NEGIR	[0.7640630, 0.7703582]	[21.6626007, 25.8950075]	[0.1959427, 0.2768060]
NLGamIR	[29.83443932, 35.20388063]	[4.23819280, 4.65152195]	[0.01511706, 0.02365754]
NBeIR	[5.9071571, 7.9709860]	[0.7335148, 0.7445871]	[1.1073351, 1.6785324]
NIR	-------	--------	[11.84369, 13.04873]

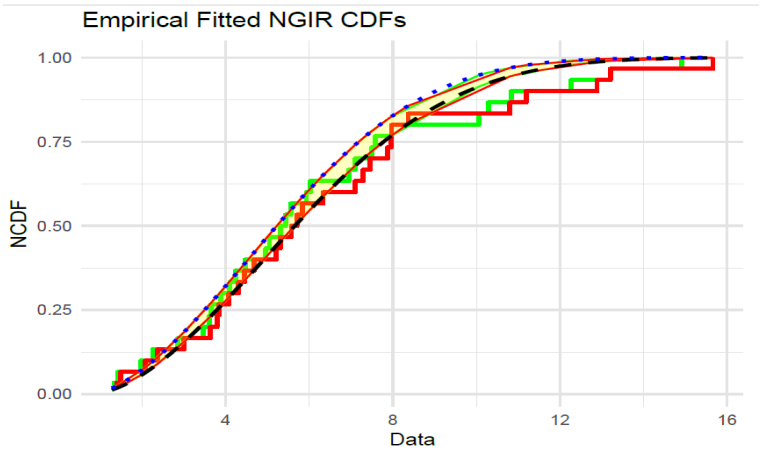

Figure 6. Empirical Fitted NGIR NCDFs with data set

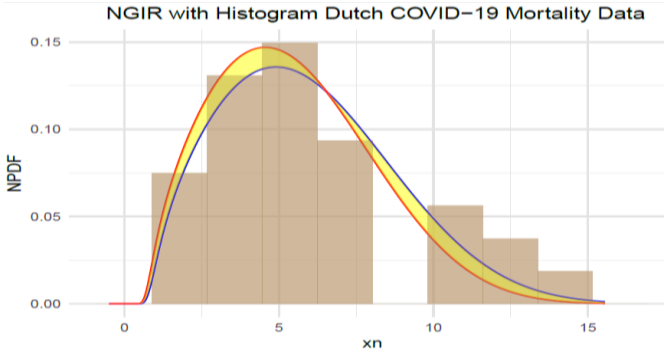

Figure 7. NGIR with Histogram Dutch COVID-19 Mortality Data

Table 4: The NGIR distribution demonstrated superior performance across the evaluated criteria, consistently yielding the lowest values among all compared models. This suggests it provides the most accurate representation of the data. For instance, its AIC values ranged between [158.7706, 159.9583], significantly lower than those of alternatives like the NOLIR distribution, which ranged from [172.9734 to 175.2927]. These results highlight the NGIR model's strength in minimizing information loss.

Table 5: Further validation of the NGIR distribution's effectiveness is found in its performance on goodness-of-fit tests. It achieved the lowest W and A statistics (e.g., W values within [0.0268702, 0.02770035]) along with th highest p-values (ranging from [0.9639576 to 0.9816981]), outperforming other models that showed weaker fits to the data.

Table 6: This table summarizes the parameter estimates obtained through the maximum likelihood estimation (MLE) method. For the NGIR model, parameter values were estimated with high precision, indicating the model's strong capacity to account for variability and uncertainty within the dataset.

Figure 6 compares the empirical cumulative distribution function (ECDF) of the observed data with the theoretical NCDF of the NGIR model. The close alignment between the two curves suggests a strong agreement, reinforcing the model's suitability for this dataset.

Figure 7 displays the data histogram overlaid with the NGIR probability density function. The alignment between the empirical and theoretical distributions further confirms the model's capability in capturing the characteristics of the COVID-19 mortality data.

CONCLUSION

The study results confirm that the NGIR provides an effective framework for modeling data with high degrees of uncertainty, such as COVID-19 mortality data. By analyzing the attached tables and figures, it is clear that the NGIR outperformed other distributions in terms of information criteria and goodness of fit, recording the lowest AIC and BIC values and the highest p-values. This indicates that the model is able to better capture the variance and uncertainty in the data.

Also, Monte Carlo simulations showed that the Maximum Likelihood (MLE) method was the most accurate in estimating the NGIR parameters compared to other methods such as the LSE and WLSE. A practical application on Dutch data confirmed the model's suitability, as its strength lies in its ability to handle parameter intervals, making it suitable for data with an ambiguous nature.

In addition, the graphs showing the convergence of the theoretical curves with the actual data support the hypothesis that the NGIR provides an accurate representation of reality. These results open new avenues for the use of neutrosophic models in the analysis of epidemiological data and other areas characterized by uncertainty. Finally, the study recommends the use of NGIR as a fundamental tool in the statistical modeling of complex data, emphasizing the importance of choosing appropriate estimation methods such as MLE to ensure the accuracy of results. It also proposes future research to explore the model's applications in other fields and expand its scope to include additional types of uncertain data.

Funding Statement: This work was supported and funded by the Deanship of Scientific Research at Imam Mohammad Ibn Saud Islamic University (IMSIU) (grant number IMSIU-DDRSP2501).

REFERENCES

A. Alzaatreh, C. Lee and F. Famoye, "A new method for generating families of continuous distributions," Metron, p. 63–79, 71 2013.

M. Bourguignon, R. B. Silva and G. M. Cordeiro, "The Weibull-G family of probability distributions," Journal of data science, pp. 53-68, 1 12 2014.

M. Alizadeh, G. M. Cordeiro, E. d. Brito and C. G. B. Demétrio , "The beta Marshall-Olkin family of distributions," Journal of Statistical distributions and Applications, pp. 1-18, 2 2015.

A. A. Al-Babtain, M. K. Shakhatreh, M. Nassar and A. Z. Afify, "A new modified Kies family: Properties, estimation under complete and type-II censored samples," Mathematics and engineering applications, p. 1345, 8 8 2020.

H. S. Klakattawi and W. H. Aljuhani, "A new technique for generating distributions based on a combination of two techniques: Alpha power transformation and exponentiated TX distributions family," Symmetry , p. 412, 3 13 2021.

S. Hussain, M. U. Hassan, M. S. Rashid and R. Ahmed, "Families of Extended Exponentiated Generalized Distributions and Applications of Medical Data Using Burr III Extended Exponentiated Weibull Distribution," Mathematics, p. 3090, 14 11 2023.

I. A. Sadiq, S. I. Doguwa, A. Yahaya and J. Garba, "New Generalized Odd Fréchet-G (NGOF-G) Family of Distribution with Statistical Properties and Applications," UMYU Scientifica, pp. 100-107, 3 2 2023.

Y. Y. Abdelall, A. S. Hassan and E. M. Almetwally, "A new extention of the odd inverse Weibull-G family of distributions: Bayesian and non-Bayesian estimation with engineering applications," Computational Journal of Mathematical and Statistical Sciences , pp. 359-388, 2 3 2024.

G. A. Mahdi, M. A. Khaleel, A. M. Gemeay, M. Nagy , A. H. Mansi, M. M. Hossain and E. Hussam, "A new hybrid odd exponential-Φ family: Properties and applications," AIP Advances, 4 14 2024.

N. A. Noori, A. A. Khalaf and M. A. Khaleel, "A New Generalized Family of Odd Lomax-G Distributions Properties and Applications," Advances in the Theory of Nonlinear Analysis and Its Application, pp. 1-16, 4 7 2023.

A. M. Abd El-latif , F. A. Almulhim, N. A. Noori, M. A. Khaleel and B. S. Alsaedi , "Properties with application to medical data for new inverse Rayleigh distribution utilizing neutrosophic logic," Journal of Radiation Research and Applied Sciences, p. 101391, 2 18 2025.

M. M. Alanaz, M. Y. Mustafa and Z. Y. Algamal, "Neutrosophic Lindley distribution with application for Alloying Metal Melting Point," International Journal of Neutrosophic Science, pp. 65-71, 4 21 2023.

K. Zahid , M. M. A. Almazah , O. H. Odhah and H. M. Alshanbari, "Generalized pareto model: properties and applications in neutrosophic data modeling. Mathematical Problems in Engineering," Mathematical Problems in Engineering, p. 3686968, 1 2022.

M. M. Alanaz and Z. Y. Algamal, "Neutrosophic exponentiated inverse Rayleigh distribution: Properties and Applications," International Journal of Neutrosophic Science, pp. 36-43, 4 21 2023.

O. E. Al-Saqal, Z. A. Hadied and Z. Y. Algamal, "Modeling bladder cancer survival function based on neutrosophic inverse Gompertz distribution," International Journal of Neutrosophic Science, pp. 75-5, 1 25 2025.

Z. Y. Algama, N. N. Alobaidi, A. A. Hamad, M. M. Alanaz and M. Y. Mustafa, "Neutrosophic Beta-Lindley distribution: Mathematical properties and modeling bladder cancer data," International Journal of Neutrosophic Science, pp. 186-194, 2 23 2024.

Z. Khan, M. M. A. Almazah, O. H. Odhah and H. M. Alshanbari, "Generalized Pareto Model: Properties and Applications in Neutrosophic Data Modeling," Mathematical Problems in Engineering, p. 3686968, 1 2022.

A. M. Almarashi, J. Farrukh , C. Chesneau and M. Elgarhy, "A new truncated muth generated family of distributions with applications," Complexity , p. 1211526, 1 2021.

A. R. El-Saeed, N. A. Noori, M. A. Khaleel and S. M. Alghamdi, "Statistical properties of the Odd Lomax Burr Type X distribution with applications to failure rate and radiation data," Journal of Radiation Research and Applied Sciences, p. 101421, 2 18 2025.

A. M. Hussien and M. A. Azher, "New SIR Model and Vaccine rate with application," NeuroQuantology , p. 3050, 7 20 2022.

A. Hassan, M. Sabry and A. Elsehetry, "A new probability distribution family arising from truncated power Lomax distribution with application to Weibull model," Pakistan Journal of Statistics and Operation Research, pp. 661-674, 2020.

H. J. Gómez, K. I. Santoro, I. B. Chamorro, O. Venegas, D. I. Gallardo and H. W. Gómez, "A Family of Truncated Positive Distributions," Mathematics, p. 4431, 21 11 2023.

K. H. Al-Habib, M. A. Khaleel and H. Al-Mofleh, "A new family of truncated nadarajah-haghighi-g properties with real data applications," Tikrit Journal of Administrative and Economic Sciences, p. 2, 61 19 2023.

A. A. Khalaf, M. A. Khaleel and N. A. Noori, "A new expansion of the Inverse Weibull Distribution: Properties with Applications," Iraqi Statistians Journal, pp. 52-62, 1 1 2024.

A. N. Nooruldeen, A. k. Mundher and D. A. Dalya , "The Modified Burr-III Distribution Properties, Estimation, Simulation, with Application on Real Data," Iraqi Statisticians Journal, pp. 225-246, special issue for ICSA2025 2 2025.

S. Rezaei, A. K. Marvasty, S. Nadarajah and M. Alizadeh, "A new exponentiated class of distributions: Properties and applications," Communications in Statistics-Theory and Methods, pp. 6054-6073, 12 46 2017.

I. A. Sadiq, S. I. S. Doguwa, A. Yahaya and A. Usman, "Development of New Generalized Odd Fréchet-Exponentiated-G Family of Distribution," A periodical of the Faculty of Natural and Applied Sciences, UMYU, Katsina, p. 169 – 178, 4 2 2023.

R. M. Mahabubur, B. Al-Zahrani and M. Q. Shahbaz, "A general transmuted family of distributions," Pakistan Journal of Statistics and Operation Research, pp. 451-469, 2018.

N. A. Noori, "Exploring the Properties, Simulation, and Applications of the Odd Burr XII Gompertz Distribution," Advances in the Theory of Nonlinear Analysis and Its Application, pp. 60-75, 4 7 2023.

S. Naz, L. A. Al-Essa, H. S. Bakouch and C. Chesneau, "A transmuted modified power-generated family of distributions with practice on submodels in insurance and reliability," Symmetry , p. 1458, 7 15 2023.

N. A. Noori and M. A. khaleel, "Estimation and Some Statistical Properties of the hybrid Weibull Inverse Burr Type X Distribution with Application to Cancer Patient Data," Iraqi Statisticians Journal, pp. 8-29, 2 1 2024.

K. N. Abdullah, N. A. Noori and M. A. khaleel, "Data Modelling and Analysis Using Odd Lomax Generalized Exponential Distribution: an Empirical Study and Simulation," Iraqi Statisticians Journal, pp. 146-162, 1 2 2025.

S. Abid and R. Abdulrazak, "[0, 1] truncated Frechet-Weibull and Frechet distributions," International Journal of Research in Industrial Engineering, pp. 106-135, 1 7 2018.

A. A. Khalaf, M. Q. Ibrahim and N. A. Noori, "[0,1]Truncated Exponentiated Exponential Burr type X Distributionwith Applications," Iraqi Journal of Science, pp. 4428-4440, 8 65 2024.

H. M. Almongy, E. M. Almetwally, H. M. Aljohani, A. S. Alghamdi and E. H. Hafez, "A new extended Rayleigh distribution with applications of COVID-19 data," Results in Physics, p. 104012, 23 2021.

H. A. Hiba , N. S. khalaf and N. A. Noori, "Comparison of non-linear time series models (Beta-t-EGARCH and NARMAX models," Iraqi Journal For Computer Science and Mathematics, p. 26–44, 3 5 2024.

N. A. Noori and A. A. Mohammad, "Dynamical approach in studying GJR-GARCH (Q, P) models with application," Tikrit Journal of Pure Science, pp. 145-156, 2 6 2021.

G. M. Cordeiro, E. M. M. Ortega and T. G. Ramires , "A new generalized Weibull family of distributions: mathematical properties and applications," Journal of Statistical Distributions and Applications, pp. 1-25, 2 2015.

Y. Wang, Z. Feng and A. Zahra, "A new logarithmic family of distributions: Properties and applications," CMC-Comput. Mater. Contin, p. 919–929, 66 2021.

F. A. Bhatti, G. G. Hamedani, M. C. Korkmaz, G. M. Cordeiro, H. M. Yousof and M. Ahmad , "On Burr III Marshal Olkin family: development, properties, characterizations and applications," Journal of Statistical Distributions and Applications, pp. 1-21, 6 2019.

N. Eugene, L. Carl and F. Famoye, "Beta-normal distribution and its applications.," Communications in Statistics-Theory and methods, pp. 497-512, 4 31 2002.

